Available online at www.elixirpublishers.com (Elixir International Journal)

Applied Mathematics

Elixir Appl. Math. 58A (2013) 15087-15093

ISSN: 2229-712X

Exact Analysis of Unsteady Convective Diffusion in a Herschel–Bulkley Fluid in an Annular Pipe

B.Ramana and G. Sarojamma

Department of Applied Mathematics, Sri Padmavati Mahila Visvavidyalayam, Tirupati, A.P., India.

ARTICLE INFO

Article history:

Received: 26 November 2012;
Received in revised form:
15 May 2013;
Accepted: 21 May 2013;

Keywords

Herschel–Bulkley Fluid,
Dispersion,
Steady flow,
Catheterized artery.

ABSTRACT

The dispersion of a solute in an annulus modeling blood as Herschel-Bulkley fluid is studied by using the generalized dispersion model. The impact of the presence of catheter and the non- Newtonian nature of blood is studied. It is observed that the yield stress and presence of catheter inhibit the rate of dispersion. The dispersion coefficient is found to be dependent on the yield stress of the fluid, the power law index of the fluid and the annular gap. The steady state value of dispersion is found to decrease in the order Newtonian, Bingham, Power law and Herschel-Bulkley fluids consecutively. The results of this model can be applied to understand the role played by the size of the catheter on the process of dispersion in a catheterized artery. A comparison of the dispersion coefficient and concentration has been made in the Newtonian, Bingham, Power law and Herschel-Bulkley fluids

Introduction

The study of longitudinal dispersion in a straight tube has applications in chromatography, environmental dynamics, biomedical engineering and physiological fluid dynamics. The insertion of a catheter into an artery forms the annular region between the catheter wall and the arterial wall. The insertion of catheter will change the flow field and disturb the hemodynamic conditions that exist in the artery before catheterization. Therefore, the recordings of the flow or the pressure gradient measured by a transducer attached to the catheter will differ from that of uncatheterized artery. Therefore, it is essential to know catheter induced errors in order to obtain the accurate readings of pressure etc. The sampling system involved in the multiple indicator dilution technique to study the blood tissue exchange induces variations in the time concentration curve and thus recorded curve is not of the same shape as the *in situ* concentration time curve evaluated at the withdrawal site, (Milner and Jose, 1960). The need for correcting the errors due to insertion of catheter are noticed and discussed in the experimental works when catheters are used for measurements (Parrish *et al.*, 1962, Cooper *et al.*, 1963, Goresky and Silverman 1963).

The dispersion of a solute in a tubular flow is studied by Aris (1959) considering two phases of flow with velocities and diffusion coefficients varying with radial distance. Sankarasubramanian and Gill (1971) analyzed the diffusion in an eccentric annular region. Tsangaris and Athanassiadis (1985) studied the dispersion of a contaminant in oscillatory flow in annular region by obtaining the effective diffusion coefficient. Rao and Deshikachar (1987) studied the unsteady convective dispersion of a solute in a solute in a fully developed flow in an annular pipe by extending the analysis of Gill and Sankarasubramanian (1970). They evaluated the dispersion coefficient as a function of time using a generalized dispersion model which is valid for all the times. The studies of Sankarasubramanian and Gill (1971) and Rao and Deshikachar (1987) revealed that the axial dispersion of mean concentration decreased with increase in the radius of the inner cylinder. Smith and Walton (1992) studied dispersion of solutes in an inclined flow in an annulus. Nagarani *et al*. (2006) studied the dispersion of a solute in a Casson fluid in an annulus using the generalized dispersion model.

It was reported (Scott Blair and Spanner (1974)) blood obeys Casson equation in a limited range. No difference between the plots of Herschel–Bulkley and Casson fluid, except at very high and very low shear rates was found when plotted using the experimental data. It is observed that the Casson fluid model can be used for moderate shear rates γ < 10/s in smaller diameter tubes whereas the Herschel– Bulkley fluid model can be used at still lower shear rate of flow in very narrow arteries where the yield stress is high (Tu et al. 1996). Further, the mathematical model of Herschel–Bulkley fluid also describes the behaviour of Newtonian fluid, Bingham fluid and power law fluid by taking appropriate values of the parameters viz. yield stress and power law index.

In this paper, an attempt has been made to analyze the dispersion of a solute in Hershel-Bulkley fluid flowing in an annular pipe, using the generalized dispersion model. The objective of this study is to apply this analysis for understanding the dispersion of an indicator and the errors in flow measurements in the cardiovascular system that arises due to the insertion of a catheter.

Mathematical Formulation

Fig 1 shows the schematic diagram of the annular geometry. The radius of the outer tube is ‘a’ and that of the inner tube is ‘ka’ with k < 1. For a fully developed, laminar flow of a Herschel-Bulkley fluid in an annulus, the non dimensional convective diffusion equation, which describes the local concentration C of a solute as a function of axial distance z, radial distance r and time t in non-dimensional form is given by

Tele:
E-mail addresses: ramana.bahunadam@gmail.com

$$\frac{\partial C}{\partial t}+w\frac{\partial C}{\partial z} = \left[\frac{1}{r}\frac{\partial}{\partial r}\left(r\frac{\partial}{\partial r}\right)+\frac{1}{Pe^2}\frac{\partial^2}{\partial z^2}\right]C \quad (1a)$$

where the non-dimensional variables are

$$C=\frac{\bar{C}}{C_0},\ w=\frac{\bar{w}}{w_0},\ r=\frac{\bar{r}}{a},\ z=\frac{D_m\bar{z}}{a^2 w_0},\ t=\frac{D_m\bar{t}}{a^2} \quad (1b)$$

C_0 is the reference concentration, w is the axial velocity of the fluid in pipe and D_m is coefficient of molecular diffusion (molecular diffusivity) which is assumed to be constant, $Pe = \frac{a\,w_0}{D_m}$ is the Peclet number.

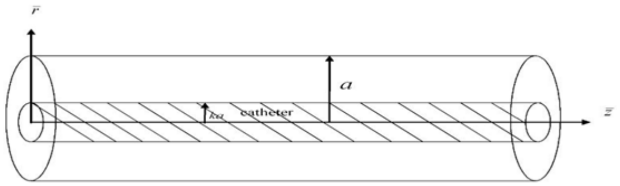

Fig1 Schematic diagram of catheterized artery

The initial and boundary conditions for the slug input of solute length z_s, in dimensionless form, are given by

$$C(0,r,z) = 1 \quad \text{if } |z| \le z_s/2 \quad (2a)$$

$$C(0,r,z) = 0 \quad \text{if } |z| > z_s/2 \quad (2b)$$

$$C(t,r,\infty) = 0 \quad (2c)$$

$$\frac{\partial C}{\partial r}(t,z,k) = 0 = \frac{\partial C}{\partial r}(t,1,z) \quad (2d, e)$$

The constitutive equation for a Herschel-Bulkley fluid relating the stress (τ) and rate of strain $\left(\frac{dw}{dr}\right)$ in the non-dimensional form is given by

$$\tau = \tau_y + \left(-\frac{dw}{dr}\right)^{1/n} \quad \text{if } \tau \ge \tau_y \quad (3a)$$

$$\frac{\partial w}{\partial r} = 0 \quad \text{if } \tau \le \tau_y \quad (3b)$$

where '*n*' is the power law index. τ_y is the non-dimensional yield stress of the fluid. The above relations between the shear stress (τ) and shear rate ($\partial w/\partial r$) are appropriate for positive values of τ and negative values of $\partial w/\partial r$. The equivalent form of these relations for more general situation, where the shear stress and shear rate can change sign may be written as (Aroesty and Gross, 1972 a, b)

$$\frac{\partial w}{\partial r} = -(\tau-\tau_y)^n \quad \text{if } \tau \ge \tau_y \quad (4a)$$

$$\frac{\partial w}{\partial r} = 0 \quad \text{if } \tau \le \tau_y \quad (4b)$$

From equation (4) it is seen that the flow of a Herschel-Bulkley fluid in an annular region has three phases such that in the central core region the velocity profile is flat and hence forms the plug flow region. In this plug flow region the shear stress does not exceed the yield stress τ_y, and the fluid does not flow by itself but is merely carried along by the fluid in the two adjacent shear flow regions as a solid body with a constant velocity – the plug flow velocity. If the plug flow region is represented by $\lambda_1 \le r \le \lambda_2$ where $k \le \lambda_1, \lambda_2 \le 1$, and the two shear flow regions by $k \le r \le \lambda_1$ and $\lambda_2 \le r \le 1$, then the Hershel-Bulkley fluid's constitutive equation (4) in these regions can be written as

$$\frac{\partial w}{\partial r} = (-\tau)^n - n\tau_y(-\tau)^{n-1}) \quad \text{if } k \le r \le \lambda_1 \quad (5a)$$

$$\frac{\partial w}{\partial r} = 0 \quad \text{if } \lambda_1 \le r \le \lambda_2 \quad (5b)$$

$$\frac{\partial w}{\partial r} = -(\tau^n - n\tau_y\tau^{n-1}) \quad \text{if } \lambda_2 \le r \le 1 \quad (5c)$$

where λ_1 and λ_2 are the yield plane locations. The velocity distribution in these regions is given by

$$w(r) = w^+(r) = P_s^n\left[\int_k^r\left(\frac{\lambda^2-r^2}{r}\right)^n dr - n\Lambda\int_k^r\left(\frac{\lambda^2-r^2}{r}\right)^{n-1}dr\right]$$

$$\text{if } k \le r \le \lambda_1 \quad (6a)$$

$$w = w^-(r) = w_p = w^+(\lambda_1) = w^{++}(\lambda_2) = \text{constant}$$

$$\text{if } \lambda_1 \le r \le \lambda_2 \quad (6b)$$

$$w(r) = w^{++}(r) = P_s^n\left[\int_r^1\left(\frac{r^2-\lambda^2}{r}\right)^n dr - n\Lambda\int_r^1\left(\frac{r^2-\lambda^2}{r}\right)^{n-1}dr\right]$$

$$\text{if } \lambda_2 \le r \le 1 \quad (6c)$$

wher $\Lambda = \lambda_2 - \lambda_1 = \tau_y/P_s$ (6d)

is the width of the plug flow region and

$$\lambda^2 = \lambda_1\lambda_2 \quad (6e)$$

and P_s is the steady state pressure gradient. The superscripts '+' and '+ +' represent the shear flow regions $k \le r \le \lambda_1$ and $\lambda_2 \le r \le 1$, respectively, and the superscript '–' represents the plug flow region $\lambda_1 \le r \le \lambda_2$. From eq (6b) and using (6d) and (6e), we obtain

$$\int_k^{\lambda_1}\left(\frac{\lambda_1(\Lambda+\lambda_1)-r^2}{r}\right)^n dr - \int_{\Lambda+\lambda_1}^1\left(\frac{r^2-\lambda_1(\Lambda+\lambda_1)}{r}\right)^n dr$$

$$-n\Lambda\int_k^{\lambda_1}\left(\frac{\lambda_1(\Lambda+\lambda_1)-r^2}{r}\right)^{n-1}dr + n\Lambda\int_{\Lambda+\lambda_1}^1\left(\frac{r^2-\lambda_1(\Lambda+\lambda_1)}{r}\right)^{n-1}dr = 0 \quad (7)$$

which is integral equation to be solved for λ_1 numerically by using Regula falsi method, and λ_2 can be obtained from equation (6d), once λ_1 is known .The mean velocity is defined as

$$w_m = \frac{\int_0^{2\pi}\int_k^1 w\,r\,dr\,d\theta}{\int_0^{2\pi}\int_k^1 r\,dr\,d\theta} = \frac{2}{1-k^2}\int_k^1 w\,r\,dr \quad (8)$$

Method of Solution

Let us consider the convection across the plane, which moves with the average velocity w_m of the fluid. For this we need to define a new co-ordinate system (r, z_1, t) with the new axial coordinate z_1 given by

$$z_1 = z - w_m t \quad (9)$$

The solution of the equation (1), together with the conditions (2) is formulated as a series expansion following Gill and Sankarasubramanian (1970), and is given by

$$C = C_m + \sum_{j=1}^{\infty} f_j(t,r) \frac{\partial^j C_m}{\partial z_1^j} \quad (10)$$

where

$$C_m = \frac{\int_0^{2\pi}\int_k^1 C\, r\, dr d\theta}{\int_0^{2\pi}\int_k^1 r dr d\theta} = \frac{2}{(1-k^2)} \int_k^1 C\, r\, dr \quad (11)$$

is the mean (average) concentration over a cross-section. On transforming the unsteady convective diffusion equation (1) into the moving co-ordinate system (r, z_1, t) where z_1 is defined by equation (9) and substituting equation (10) into the transformed unsteady convective diffusion equation, we obtain

$$\frac{\partial C_m}{\partial t} + (w-w_m)\frac{\partial C_m}{\partial z_1} - \frac{1}{Pe^2}\frac{\partial^2 C_m}{\partial z_1^2} + \sum_{j=1}^{\infty}\left[\left(\frac{\partial f_j}{\partial t} - \frac{1}{r}\frac{\partial}{\partial r}(r\frac{\partial f_j}{\partial r})\right)\frac{\partial^j C_m}{\partial z_1^j} + (w-w_m) f_j \frac{\partial^{j+1} C_m}{\partial z_1^{j+1}} - \frac{1}{Pe^2} f_j \frac{\partial^{j+2} C_m}{\partial z_1^{j+2}} + f_j \frac{\partial^{j+1} C_m}{\partial t\, \partial z_1^j}\right] = 0 \quad (12)$$

It is assumed that the process of distributing C_m is diffusive in nature from the time 'zero', then as in Gill and Sankarasubramanian (1970) the generalized dispersion model for C_m can be written as

$$\frac{\partial C_m}{\partial t} = \sum_{i=1}^{\infty} K_i(t) \frac{\partial^i C_m}{\partial z_1^j} \quad (13)$$

with dispersion coefficients K_i as suitable functions of time t. The first two terms on the right hand side of equation (13) describe the transport of C_m in axial direction z_1 through convection and diffusion respectively, and therefore the coefficients K_1 and K_2 are termed as the longitudinal convection and diffusion coefficients for C_m respectively.

Substituting equation (13) in equation (12) and rearranging the terms, we get

$$\sum_{i=1}^{\infty} K_i(t) \frac{\partial^i C_m}{\partial z_1^i} + (w-w_m)\frac{\partial C_m}{\partial z_1} - \frac{1}{Pe^2}\frac{\partial^2 C_m}{\partial z_1^2} + \sum_{j=1}^{\infty}\left\{(\frac{\partial f_j}{\partial t} - \frac{1}{r}\frac{\partial}{\partial r}(r\frac{\partial f_j}{\partial r}))\frac{\partial^j C_m}{\partial z_1^j} + (w-w_m) f_j(t,r)\frac{\partial^{j+1} C_m}{\partial z_1^{j+1}} - \frac{1}{Pe^2} f_j(t,r)\frac{\partial^{j+2} C_m}{\partial z_1^{j+2}} + f_j(t,r)\sum_{i=1}^{\infty} K_i(t)\frac{\partial^{i+j} C_m}{\partial z_1^{i+j}}\right\} = 0 \quad (14)$$

Comparing the coefficients of $\frac{\partial^j C_m}{\partial z_1^j}$, j = 1, 2, .. , we get an infinite set of differential equations given by

$$K_1(t) + \frac{\partial f_1}{\partial t} - \frac{1}{r}\frac{\partial}{\partial r}(r\frac{\partial f_1}{\partial r}) + (w-w_m) = 0 \quad (15)$$

$$K_2(t) - \frac{1}{Pe^2} + \frac{\partial f_2}{\partial t} - \frac{1}{r}\frac{\partial}{\partial r}(r\frac{\partial f_2}{\partial r}) + [(w-w_m) + K_1(t)]\, f_1 = 0 \quad (16)$$

$$K_{j+2}(t) + \frac{\partial f_{j+2}}{\partial t} - \frac{1}{r}\frac{\partial}{\partial r}(r\frac{\partial f_{j+2}}{\partial r}) + (w-w_m) f_{j+1} - \frac{1}{Pe^2} f_j + \sum_{i=1}^{j+1} K_i(t) f_{j+2-i} = 0 \quad (17)$$

for j = 1, 2… with $f_0 = 1$.

Since C_m can be chosen to satisfy the initial condition on *C*, the initial and boundary conditions on f_j's can be obtained from equations (2), we have

$f_j(0, r) = 0 \quad j = 1, 2….$ (18a)

$$\frac{\partial f_j}{\partial r}(t, k) = 0 = \frac{\partial f_j}{\partial r}(t, 1) \quad j = 1, 2,….. \quad (18b)$$

and from equations (10) and (11), we have $\int_k^1 f_j\, r\, dr = 0$ j = 1, 2,… (19)

Multiplying equations (15), (16) and (17) by r and integrating from k to 1, by using the condition (19) we get

$$K_1(t) = -\frac{2}{1-k^2}\int_k^1 (w-w_m)\, r\, dr = 0 \quad (20)$$

$$K_2(t) = \frac{1}{Pe^2} - \frac{2}{1-k^2}\int_k^1 f_1(t,r)\; w(r)\; r\, dr \quad (21)$$

$$K_{j+2}(t) = -\frac{2}{1-k^2}\int_k^1 f_{j+1}(t,r)\, w(r)\; r\, dr,$$

for j = 1, 2… (22)

Using (20), equation (15) takes the form

$$\frac{\partial f_1}{\partial t} - \frac{1}{r}\frac{\partial}{\partial r}(r\frac{\partial f_1}{\partial r}) + (w-w_m) = 0 \quad (23)$$

The function f_1 is the most important coefficient of the series in equation (10). It gives the measure of deviation of the local concentration C from the mean concentration C_m. The solution to the non-homogeneous parabolic partial differential equation (23) and conditions (18) and (19) can be written in the form

$f_1(t, r) = f_{1s}(r) + f_{1t}(t, r)$ (24)

where f_{1s} is the large time solution and f_{1t} is the transient part which describes the time-dependent nature of the dispersion phenomenon. Substituting (24) in equation (23) we obtain

$$\frac{1}{r}\frac{\partial}{\partial r}(r\frac{\partial f_{1s}}{\partial r}) = (w_m - w) \quad (25)$$

$$\frac{\partial f_{1t}}{\partial t} = \frac{1}{r}\frac{\partial}{\partial r}(r\frac{\partial f_{1t}}{\partial r}) \quad (26)$$

The corresponding boundary conditions on f_{1s} and f_{1t} are

$$\frac{df_{1s}}{dr}(r=k) = 0 = \frac{df_{1s}}{dr}(r=1) \quad (27a)$$

$$\frac{\partial f_{1t}}{\partial r}(t,k) = 0 = \frac{df_{1t}}{dr}(t,1) \quad (27b)$$

$f_{1t}(0, r) = -f_{1s}(r)$ (27c)

Condition (19), takes the form

$$\int_0^1 f_{1t}\; r\, dr = -\int_0^1 f_{1s}\; r\, dr = 0 \quad (28)$$

The solution for f_{1t} is obtained from the equation (26) subject to the conditions (27), and is given by

$$f_{1t} = \sum_1^{\infty} \frac{A_j}{J_1(\mu_j k)} E_0(\mu_j r)\, e^{-\mu_j^2 t} \quad (29)$$

where

$$E_0(\mu_j r) = J_1(\mu_j k) Y_0(\mu_j r) - Y_1(\mu_j k) J_0(\mu_j r) \quad (30)$$

$$A_j = -J_1(\mu_j k)\frac{\int_k^1 f_{1s} E_0(\mu_j r)\, r\, dr}{\int_k^1 r E_0^2(\mu_j r)\, dr} \quad (31)$$

and μ_j's are the solutions of the equation

$$J_1(\mu_j k) Y_1(\mu_j) - Y_1(\mu_j k) J_1(\mu_j) = 0 \quad (32)$$

where J_0, J_1 and Y_0, Y_1 are the Bessel functions of first kind and second kind of order zero and one respectively.

In the generalized dispersion model given by equation (13), K_2 plays an important role. From the equation (21), we can see that it depends on the function f_1. We can solve the equation (21) for K_2 by substituting the expression for f_{1s} and f_{1t}. Once K_2 (t) is known, then f_2 (t, r) can be obtained in a similar manner to that f_1(t, r). In this way we can find K_3 (t), f_3 (t, r), K_4 (t), f_4 (t, r) ………and so on. Since the expression for f_1 (t, r) and K_2 (t) are complex in nature, it is very difficult to evaluate f_2 (t, r), K_3 (t), ….. and so on. But for dispersion in a Newtonian fluid which corresponds to $\tau_y = 0$ and n = 1, it was shown that K_3 ($t \to \infty$)=-1/ 23040 (Gill and Sankarasubramanian,1970), and the magnitude of higher order coefficients decrease further. Owing to the yield stress and power law index these coefficients may decrease further in magnitude and hence they are not evaluated. Neglecting $K_3(t)$ and higher order coefficients, the generalized dispersion model leads to

$$\frac{\partial C_m}{\partial t} = K_2(t)\frac{\partial^2 C_m}{\partial z_1^2} \qquad (33)$$

The initial and boundary conditions for C_m are given by

$$C_m(0, z_1) = 1 \quad if \quad |z_1| \le z_s/2 \qquad (34a)$$

$$C_m(0, z_1) = 0 \quad if \quad |z_1| > z_s/2 \qquad (34b)$$

$$C_m(t, \infty) = 0 \qquad (34c)$$

The solution of the mean concentration for equation (33) with the help of the conditions (34) is given by

$$C_m = \frac{1}{2}\left[erf\left(\frac{(z_s/2)-z_1}{2\sqrt{\xi}}\right) + erf\left(\frac{(z_s/2)+z_1}{2\sqrt{\xi}}\right)\right] \qquad (35)$$

where

$$\xi = \int_0^t K_2(t)\,dt \qquad (36)$$

Results And Discussion

In this paper the dispersion of a solute in a Herschel-Bulkley fluid flowing in an annular pipe is analyzed using generalized dispersion model. Consequently the effective diffusion coefficient K_2 which describes the total dispersion process in terms of a simple diffusion process as a function of time can be evaluated. It is observed that the dispersion coefficient K_2 is influenced by the yield stress of the fluid, power law index. Further the dispersion is likely to be affected by the presence of a concentric tube. The effect of power law index on K_2 is analyzed. The results are compared and found to be in agreement with those of Rao *et al*. (1987) in the absence of yield stress τ_y = 0, n = 1 and to reduce to those of Gill and Sankarasubramanian (1970) when τ_y = 0, k $\to$ 0 and n =1. The results are discussed for different fluids Newtonian (τ_y = 0, n = 1), Power law (τ_y = 0, n = 2), Bingham ($\tau_y \neq 0$, n = 1) and Herschel-Bulkley fluids ($\tau_y \neq 0$, n = 2).

In the present study the ratio of the radius of inner tube to that of the outer tube is taken to range from 0.1 to 0.5, yield stress in the range 0.1 to 0.3 and the length of the slug input of the solute is varied from 0.004 to 0.02. For Herschel-Bulkley and power law fluids the power law index n is taken as 2. For each value of k, the associated eigen value μ_j, for j = 1, 2…… are evaluated from the equation (30) using standard root finding numerical procedure.

The dispersion coefficient K_2 in the case of a Herschel-Bulkley fluid (from which $1/Pe^2$ is deducted) versus time for different values of yield stress τ_y is described in fig 2. It is noticed that the dispersion coefficient K_2 increases significantly for small values of time and attains essentially a constant value for large values of time**.** The time taken to reach the steady state is observed to be dependent on the values of yield stress. As yield stress increases this critical value is seen to be decreasing. A similar observation is made in the case of Casson fluid by Dash *et al*. (2000) in tubular flow and Nagarani *et al*. (2006) in an annular flow.

Fig 3 shows the dispersion coefficient versus time in the Newtonian, Power law, Bingham, Herschel-Bulkley fluids. Since the velocities reduce due to the non – Newtonian nature of the above fluids in the order mentioned, a reduction in the dispersion coefficient is also noticed in the same order.

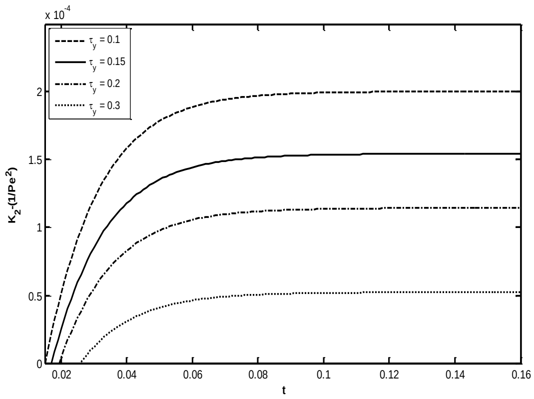

Fig 2 Variation of dispersion coefficient ($K_2 - 1/Pe^2$) with t when k = 0.2 for different values τ_y when n = 2

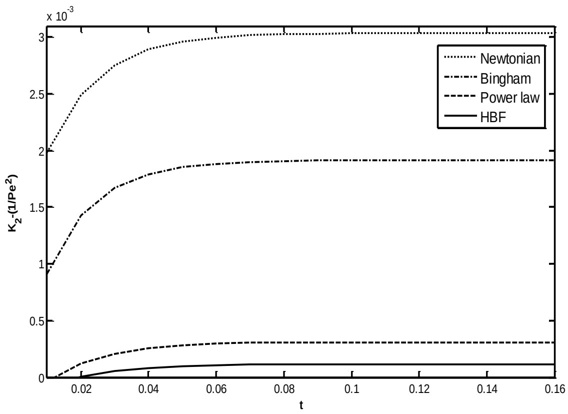

Fig 3 Variation of dispersion coefficient ($K_2 - 1/Pe^2$) with t when k = 0.2 different fluids

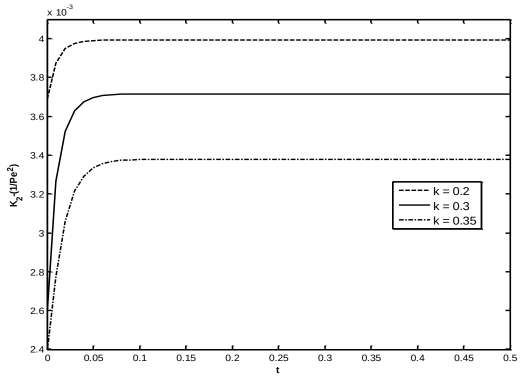

Fig 4 Variation of dispersion coefficient ($K_2 - 1/Pe^2$) with t for different values k when τ_y = 0.1, n = 2

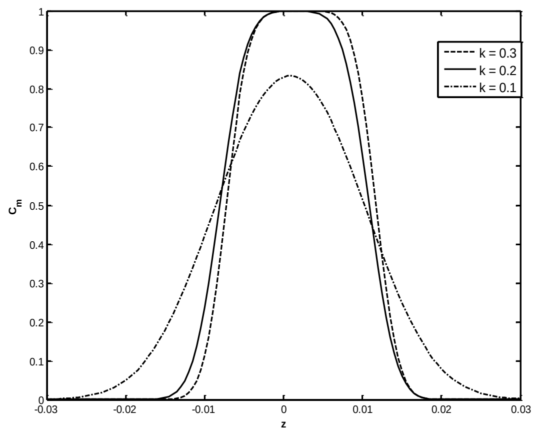

Fig 5 Variation of mean concentration C_m with axial distance z for different values k when t = 0.03, τ_y = 0.1, z_s = 0.019, Pe = 1000, n =2

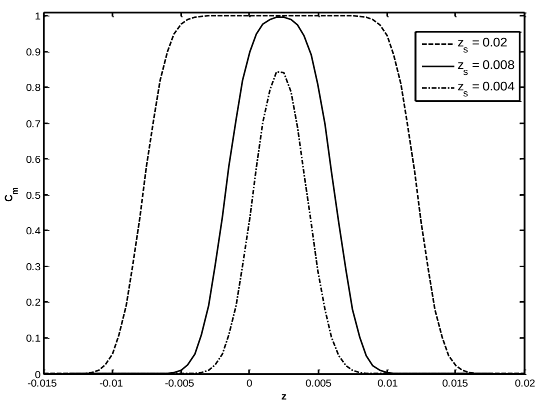

Fig 6 Variation of mean concentration C_m with axial distance z for different values z_s when t = 0.03, τ_y = 0.1, Pe = 1000, k =0.1, n = 2

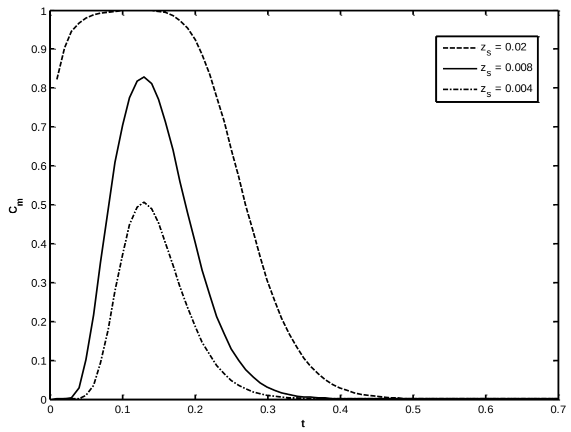

Fig 7 Variation of mean concentration C_m with t for different values z_s when z = 0.01, τ_y = 0.1, Pe = 1000, k = 0.1, n = 2

It is observed from fig 4 that reduction in the annular gap inhibits the dispersion process for all times which is also noticed by Rao and Deshikachar (1987). In case of Herschel-Bulkley fluid when yield stress is 0.1 and k varies in the range (0.2 - 0.3) the reduction factor in the dispersion coefficients varies in the range (0.0037- 0.0029)

The mean concentration versus the axial distance for various values of the annular gap is plotted in fig 5. It is observed that in a Herschel-Bulkley fluid the peak values of mean concentration occur at the origin for k = 0.1. As k increases (i.e. the annular gap reduces) the concentration profile becomes blunt and further its magnitude increases. In other words the axial dispersion decreases with increase in the radius of the inner cylinder.

The variation of C_m with axial distance z for Herschel-Bulkley fluid (with yield stress τ_y = 0.1 and k = 0.1) for various lengths of slug input of the solute is shown in fig 6. The peak concentration is found to increase from 0.8431 to 1 when the length of the slug input solute varies from 0.004 to 0.02. It is observed that the solute disperses faster when length of the slug input of solute is smaller. Fig 7 presents the mean concentration versus time for different lengths of the slug input. As the length of the slug input increases it is observed that peak values of C_m increases.

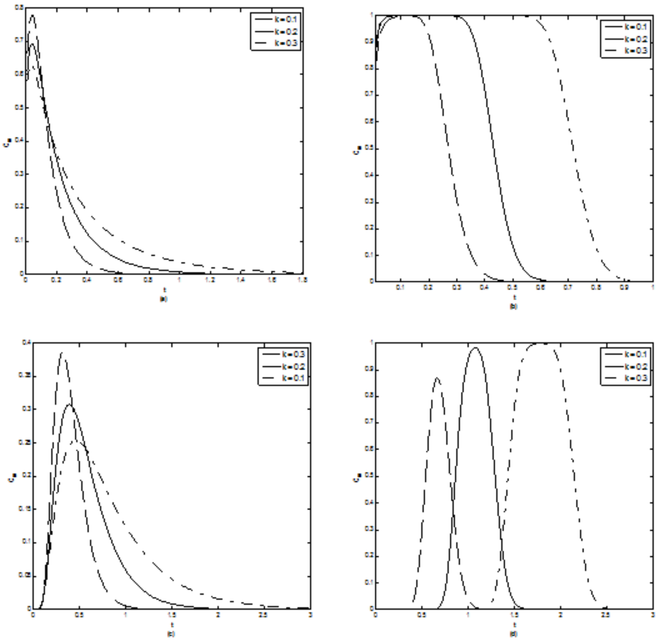

Fig 8 Variation of mean concentration C_m with t for different values k when Pe = 1000, z_s = 0.019, n = 2 (a) τ_y = 0, z = 0.01 (b) τ_y = 0.1, z = 0.01 (c) τ_y = 0, z = 0.05 (d) τ_y = 0.1, z = 0.05

In fig 8 (a, c) the observation point is just outside the slug while in fig 8 (b, d) it is at farther distance from the slug. For Newtonian fluid fig (8a) the peak values of the concentration for different values of k are attained in a smaller interval of time (0.42-0.5) while in the case of Herschel-Bulkley fluid the peak values occurred in the interval (0.6, 1.8). In the Newtonian case the peak value of concentration increases from 0.25 to 0.38 when k changes from 0.1 to 0.3 while in the Herschel-Bulkley fluid case it changes from 0.86 to 0.99. Fig 9 (a, b) shows the mean concentration against axial distance for Newtonian and Bingham fluids, and power law and Herschel Bulkley fluids. It is observed that the axial dispersion decreases due to the non-Newtonian nature of the fluid. Fig 10(a, b) describes the mean concentration against time for Newtonian and Bingham fluids, and Power law and Herschel-Bulkley fluids. It is noticed from fig 10(a) that the mean concentration attains its peak value earlier than that of the Bingham fluid. Similarly fig 10(b) shows that the peak value of mean concentration attains much faster (t = 0.45) in Power law fluids than in Herschel-Bulkley fluid (0.68).

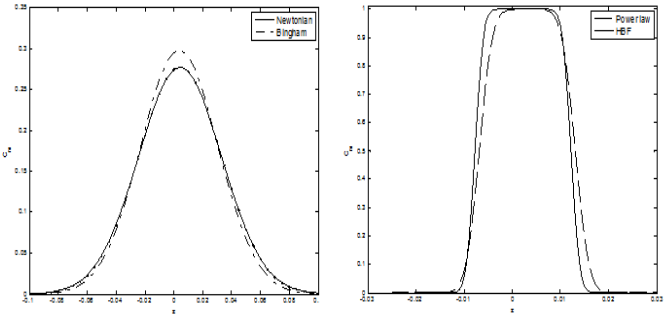

Fig 9 Variation of mean concentration C_m with axial distance z for different fluids when k =0.1, z_s = 0.02, t = 0.3

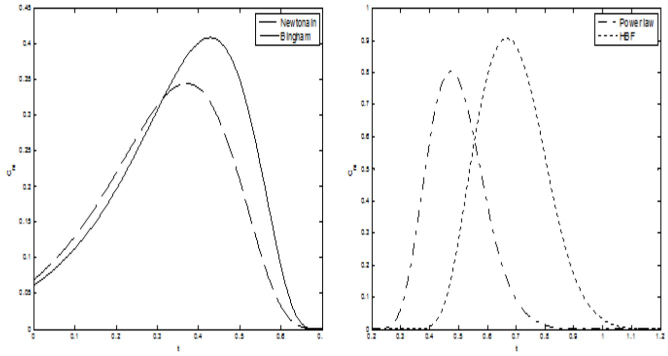

Fig 10 Variation of mean concentration C_m with t for different fluids when k = 0.1, z_s = 0.02, z = 0.05

Applications To Catheterized Artery

The analysis of this mathematical model can be applied to understand the dispersion of an indicator in a catheterized artery of radius '*a'* and catheter of radius ka which is inserted coaxially. The objective is to estimate the catheter induced error in the measured values based on the concept of longitudinal dispersion of substance due to the combined action of the convection and the diffusion. The ratio of the radius of the catheter to that of the artery (k) is varied from 0.1 to 0.3 to understand the impact of the size of the catheter on the mass transport process. The values of the yield stress are varied from 0.1 to 0.3. The variation of K_2 versus k for different values of yield stress is described in table 1.

Table 1 Variation of effective diffusivity coefficient for steady state dispersion with catheter radius (k) and yield stress (τ_y) of the fluid

	$\tau_y = 0$	$\tau_y = 0.1$	$\tau_y = 0.2$	$\tau_y = 0.3$
k = 0	5.21×10^{-3}	4.58×10^{-3}	2.41×10^{-3}	2.67×10^{-4}
k = 0.1	4.56×10^{-3}	6.25×10^{-4}	5.32×10^{-4}	1.86×10^{-4}
k = 0.2	2.77×10^{-3}	2.84×10^{-4}	1.14×10^{-4}	5.23×10^{-5}
k = 0.3	1.45×10^{-3}	4.91×10^{-5}	2.41×10^{-5}	1.25×10^{-5}

It is seen from the table that presence of a catheter reduces the dispersion when the annular gap is 0.1. Further it decreases with the size of the catheter. In Newtonian fluid when the annular gap is 0.3, due to insertion of a larger catheter there is a fourfold reduction in dispersion coefficient. Further increase in the value of yield stress reduces the dispersion coefficient more. When the yield stress of the fluid is τ_y = 0.3, it is noticed that dispersion coefficient reduces five times that of the Newtonian case.

The combined effect of yield stress and size of the catheter on coefficient of dispersion is significant. It is noticed that the dispersion coefficient in the presence of large catheter (annular gap k = 0.3 and yield stress τ_y = 0.3) is reduced by four hundred times of the Newtonian case in the absence of a catheter.

Conclusions

Dispersion of a solute in an annular region in a Herschel-Bulkley fluid is analyzed employing the generalized dispersion model. Thus, the effective diffusion coefficient describes the entire dispersion process in terms of a simple diffusion processes. The dispersion coefficient is dependent on yield stress of the fluid, power law index of the fluid and the annular gap. In fact, it is observed that the yield stress and presence of a catheter inhibits the rate of dispersion. The dispersion coefficient is observed to be decreasing due to the non- Newtonian nature. The steady state value of dispersion is found to decrease in Newtonian, Bingham, Power law and Hershel-Bulkley fluids consecutively. The peak value of the mean concentration increases from 0.83 to 0.99 when k increases from 0.1 to 0.3 when τ_y = 0.1, z_s = 0.019 at t =0.03 in Herschel-Bulkley fluid.

The analysis of this model can be applied to understand the role played by the size of the catheter when inserted into an artery and the effect of non-Newtonian nature of the fluid. The insertion of a catheter of small size $k = 0.1$ leads to a five fold reduction in the dispersion coefficient to that of the corresponding value in an uncatheterized artery when blood is modeled as a Hershel-Bulkley fluid (i.e. τ_y = 0.1, n = 2). The combined effect of non-Newtonian rheology and the insertion of a catheter in an artery on the dispersion coefficient are to reduce the effective dispersion coefficient significantly.

References

Aroesty, J. and J.F. Gross (1972a), The mathematics of pulsatile flow in small blood vessels, I. Casson theory, *Microvasc. Res.* 4, 1-12.

Aroesty, J. and J.F. Gross (1972b), Pulsatile flow in small blood vessels I. Casson theory, *Biorheology* 9, 33-42.

Cooper K., J. R. Schkert, T. G. Arnold and W. W. Lacy (1963), Removal of distortion from indicator-dilution curves with analog computer, *Circ. Res*. 12, 131-137

Dash, R. K., G. Jayaraman and K.N. Mehta (2000), Shear augmented dispersion of a solute in a Casson fluid flowing in a conduit, Annals *of Biomed. Engg.* 28, 4: 373-385.

Gill, W. N. and R. Sankarasubramanian (1970), Exact analysis of unsteady convective Diffusion, *Proc. Roy. Soc. Lond. A* 316, 341-350

Goresky, C.A. and M. Silverman (1963) Effect of correction of catheter distortion on calculated liver sinusoidal volumes, *Am. J. Physiol.* 207, 883-892

Milnor, W.R. and A.D. Jose (1960) Distortion of indicator-dilution curves by sampling systems, *J. Appl. Physiol.* 15, 177-180.

Nagarani, P., G. Sarojamma and G. Jayaraman (2006) Exact analysis of unsteady convective diffusion in Casson fluid flow in an annulus – Application to catheterized artery, *Acta Mechanica* 187, 189-202

Parrish, D., G.E. Gibbons and J.W. Bell (1962) A method for reducing the distortion produced by catheter sampling systems, *J. Appl. Physiol.* 17, 369-371.

Rao., A.R. and K.S. Deshikachar (1987), An exact analysis of unsteady connective diffusion in an annular pipe, *ZAMM* 67, 189-195

Sankarasubramanian, R. and W. N. Gill (1971), Taylor diffusion in laminar flow in an eccentric annulus, *Int. J. Heat Mass Transfer* 14, 905-919

Scott Blair, G.W. and D.C. Spanner (1974), An Introduction to Biorheology, *Elsevier Scientific Publishing Company*, Amsterdam, pp. 51.

Smith, R and I. Walton (1992), A burgers concentration dispersion equation, *J. Fluid Mech.* 239, 65-80.

Tsangaris, S. and N. Athanassiadis (1985), Diffusion in oscillator flow in an annular pipe, *ZAMM* 65, 252.

Tu, C., and M. Deville (1996), Pulsatile flow of non-Newtonian fluids through arterial stenosis, *J. Biomech.* 29, 899–908.